Doc No:	SC2/ANA/S210/005
Vers:	1.11
Category:	Report
Doc Type:	LaTeX
State:	Issued
Author:	Douglas Scott & Alex van Engelen
Date:	2005/05/25

SCAN Mode Strategies for SCUBA-2

1 Introduction

This document summarizes some basic scan strategy concepts for SCUBA-2, providing 4 concrete examples of how SCUBA-2 could be used in SCAN mode: Boustrophedon; Lissajous; Pong; and Daisy. Each of these SCAN mode variations will have parameters which can be set based on the observer's requirements, as well as telescope and instrumental constraints. The plans for reducing SCAN mode data are described in an accompanying document (SC2/ANA/S210/006).

2 SCUBA-2 observing modes

As well as direct imaging, SCUBA-2 will have polarimeter and FTS capabilities. In this document we will be focussing on the strategies for continuum imaging of the I Stokes parameter, i.e. direct imaging alone.

There are 3 different observing modes planned for SCUBA-2,[4] namely STARE, DREAM and SCAN. The first (STARE) involves no movement on the sky, and no reduction steps, except for glitch-removal and 'flat-fielding'. Successful implementation of this mode requires that the detectors are extremely stable and uncorrelated. The second mode (DREAM) involves small rapid cycles by the secondary mirror and the subsequent reconstruction of the image in the presence of varying atmospheric emission, and is described elsewhere.[8] One potential problem with moving the secondary is that the effects of the changing illumination pattern may need to be modelled very accurately. It is also unclear how easy it will be to deal with any partially correlated bolometers within the DREAM reconstruction. The third approach (SCAN) involves continuously scanning the detector array across the sky through the movement of the primary dish, and it is the details of this mode which are described in this document.

The Dutch Real-Time Acquisition Mode (DREAM)[9,12] was originally envisioned as the primary imaging mode for SCUBA-2. It has always been planned that some sort of SCAN mode will be used for large images,[5] where one is interested in preserving information on the largest scale modes. DREAM may well be effective for making maps whose size is on the scale of the SCUBA-2 array ($\sim 7 \times 7$ arcmin). However, this novel observing (and reduction) mode was not successfully demonstrated using SCUBA, and its application to SCUBA-2 can only be partially tested using simulations.[6,7] Hence the extent to which DREAM works in practice may ultimately only be known after the installation of SCUBA-2 at the JCMT. To mitigate this risk we need to implement a set of SCAN mode options for SCUBA-2 at the JCMT. This applies to images which are only a little larger than the SCUBA-2 array, as well as for much larger maps.

3 Criteria for effective map-making

A fundamental principle of observing with arrays of detectors at millimetre wavelengths is that one should move detector elements over the sky at least as rapidly as the sky is changing. Another ingredient of a successful scanning strategy is that there should be sufficient 'cross-linking' in the scan pattern. If these two rules are followed, then one should be able to distinguish temporal variations (mainly rapidly varying atmospheric emission and gain fluctuations) from spatial variations (i.e. the astronomical structures which are being mapped). There is hard empirical evidence (particularly from experience with the SHARC-II array on the CSO[3]) that continuous scanning is indeed an efficient method for taking data with a total power bolometer array.

One can write down a more complete list of features which are desirable for ensuring that a SCAN mode is going to be effective:

1. Move across the sky as rapidly as possible, subject to telescope constraints.
2. Take data at a rate which is much faster than the atmosphere is changing.
3. Minimize any gaps in the data timestreams in order to preserve the integrity of the noise correlations (although any poorly characterized sections of data can be flagged so as not to be used for image reconstruction).
4. Maximize the number of detectors which see a given sky pixel (this is crucial to constraining the map solution, particularly in the presence of problems with real-world instruments, such as bad detectors, correlated noise and gain fluctuations).
5. Pass through pixels in several different directions, in order to separate temporal and spatial structures. In the presence of $1/f$-like drifting signals (as we expect for both atmospheric emission and internal detector noise) simulations have shown[13, 11] that the pixel correlation solution for the 'Least Squares' map is best constrained when the scans pass through the sky pixels in quite different directions.
6. Try to avoid a pattern which repeats so exactly that the same spatial part of the map is visited at periodic time intervals (since this may make it hard to separate genuine astronomical structure from effects in the timestreams).
7. Give close to uniform sky coverage (although this is certainly not precisely necessary and there is a compromise to be made with respect to turning around at the edges of a map).
8. Be easy to parameterize in terms of telescope motion.
9. Allow for data reduction which is tractable with reasonable computational resources.

Note that the basic 'On-The-Fly' or 'raster' mapping approach satisfies very few of these criteria. What is normally meant by 'On-The-Fly' is based on mapping a source of finite extent by comparing the 'on' data with the 'off' data – this effectively modulates the data on the timescale between 'offs', while cross-linking essentially modulates on the timescale between which individual detectors see a given sky pixel.

Several of the above criteria can be summarized in the general maxim (promoted by Ned Wright) that 'you should maximize the number of levels of modulation'. As well as these general principles, there are several choices to make in the details of how to scan the telescope. These details will depend on many factors: constraints from the telescope; the atmospheric $1/f$ knee frequency; gain variations and other properties of the detectors; the size of the region to be mapped; the range of spatial frequencies expected in the image; the strength of the desire for uniform coverage; and possibly other issues specific to individual observing programmes.

Because of these issues it is important to have a range of options available for SCUBA-2, which cover the scope of reasonable possibilities. The SCAN modes we describe below are drawn from ideas which have already been explored at other telescopes.

4 Proposed SCAN modes

There are 4 basic variations on scanning which should be implemented for use with SCUBA-2. Although they are treated separately here, they can also all be considered as just being different variations on how to drive the telescope with some $x(t)$ and $y(t)$.

4.1 Boustrophedon SCAN

The simplest form of scanning one might imagine is represented in Fig. 1, and is often referred to as the 'boustrophedon' pattern (from the Greek meaning 'turning like an ox when ploughing'). The figure shows a particularly simple example of mapping a square region in a direction parallel to one of the sides of the square. One can easily implement the same approach while scanning at some other orientation (and typically SCUBA-2 will be scanning an RA,Dec box in Naysmith coordinates). This is essentially the pattern used in many telescopes to implement an 'On-the-Fly' (OTF) raster mapping mode, and is the SCAN mode used for SCUBA (except that for SCUBA the mode has the undesirable feature of not taking data continuously, and in fact having timestream gaps at the turnaround points which are roughly equal in length to the time taken on each 'swath').

This scanning strategy satisfies many of the criteria listed above, *except* that it does not provide cross-linking of the data, and if the pattern is repeated each part of the map will be revisited on exactly the same timescale. The first objection can be partly overcome by repeating the whole process with a 90° rotation. However, this still does not entirely overcome the objection that is may still be hard to distinguish spatial structure from temporal effects in the data because a single period is built into the way the data are taken.

Nevertheless, this is such a simple scheme that it should be implemented as an option for SCUBA-2 scanning. The 'drop' at the end of each 'swath' can clearly be set so that there is a different amount of overlap between adjacent swaths. It will be desirable to ensure that each part of the sky is covered on at least 2 such sweeps (for redundancy and cross-checking), and hence the size of the 'drop' should be no more than half the array size. The optimal amount of overlap will depend on the level of systematics that exist in the data, as well as the desired speed for covering the entire map.

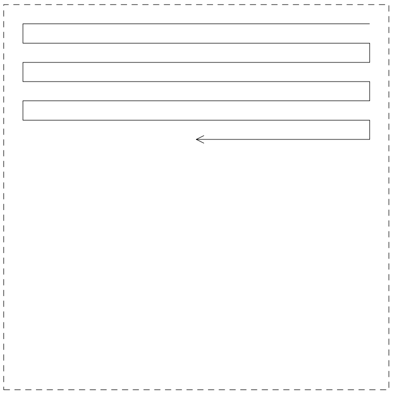

Figure 1: An example of the 'Boustrophedon' scan pattern. The telescope is mapping the region outlined with the dashed line, which is done starting at the top right-hand corner and sweeping back and forth across the map, dropping by a fixed amount at the end of each 'swath'. A more general boustrophedon pattern will be oriented at some angle to the edges of the map region.

It is obviously not necessary to have sharp corners on the Boustrophedon pattern. So one can easily imagine rounding off the turns and/or slowing down the telescope motion near the turns in order to keep within limits on telescope acceleration and jerk. (which will depend on position on the sky of course). Provided there is reliable information about pointing at all times there is no significant effect on the quality of the image; slowing down near the turns simply means somewhat lower noise near the edges of the image. If the position is not well known near the turnaround points, then those data can be flagged so they can be neglected in the map-making procedure, leading to higher noise near the edges.

4.2 Lissajous SCAN

One basic idea to interconnect sky pixels is a simple Lissajous pattern, where, e.g., for localized flat-sky map co-ordinates,

$$\begin{aligned} x(t) &= x_0 \sin(\omega t) \\ \text{and} \quad y(t) &= y_0 \sin(a\omega t), \end{aligned} \tag{1}$$

for some amplitudes x_0 and y_0, and a scalar a whose value is the ratio of the frequencies in the two directions. The pattern is periodic if and only if a is a rational number. The values of the frequencies of course need to be chosen so as not to cause any resonances in the mechanical system. This mode is effective for making relatively small maps (where it can provided an alternative to DREAM) and has been implemented at the CSO[2] as the recommended method for making small images with SHARC-II.

From an idealized mapping perspective (i.e. ignoring the constraints imposed by the telescope), the maximum scanning speed for SCUBA-2 is the product of the sampling rate and

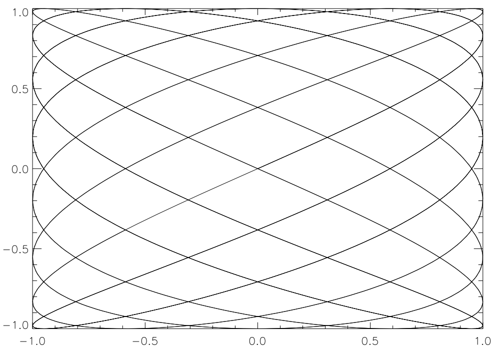

Figure 2: A sample Lissajous scan. This was generated with $a = 5/8$: note the five 'lobes' along the horizontal direction and eight 'lobes' along the vertical direction. In practice this ratio could be scaled so that at the centre of the image, the separation between adjacent 'swaths' is related to the detector separation and array size. A standard amplitude for the oscillations would be set by making this distance, for example, half the size of a SCUBA-2 subarray, i.e. $\simeq 4\,$arcmin.

the desired map resolution, which is related to the beam size via a Nyquist criterion. Differentiating the above equations, and taking $3\,$arcsec pixels for adequate resolution of the $450\,\mu$m data (which means a maximum scan rate of $600\,arcsec\,\mathrm{s}^{-1}$), we find that ω, a, x_0 and y_0 should be chosen such that

$$\omega\sqrt{x_0^2 + a^2 y_0^2} < (200\,\mathrm{Hz})(3\,\mathrm{arcsec}) = 600\,\mathrm{arcsec}\,\mathrm{s}^{-1}. \tag{2}$$

If the scanning rate is higher than this, the beam will be smeared along the scan direction (although an increase of a factor of 2 is possible if one is prepared to sacrifice resolution of the $450\,\mu$m data).

Fig. 3 shows a simulation of an example Lissajous scan pattern, with the pixel hit counts indicated as a function of time.

Choosing a rational number for a makes sense, because this causes the field to be covered by a single detector to a reasonable uniformity in a predictable amount of time (however, at some level this does not matter because of the large array size). As can be seen in Fig. 2, the number of 'lobes' along each side is given by the numerator and denominator of the rational fraction a.

A drawback to using a single sinusoidal function in each direction is the fact that more time is spent at the edges of the map than at the centre. Of course the motion at the edges must be constrained by the finite telescope acceleration, and hence in practice it may be necessary to go slower near the turnaround points, which will tend to reduce the uniformity of the map (although probably only by a modest amount). One can easily imagine choosing some other smooth, periodic function for the motion in the x- and y- directions. As an illustration of this Fig. 4 shows the sky coverage obtained by adding more Fourier modes in the expansion of a triangle wave. As more modes are added, more time is spent at the centre of the map. This somewhat mitigates the potential need to slow down near the turnaround points.

The Lissajous pattern satisfies essentially all the criteria listed at the beginning of this report. Pixels in the final map are visited by many detectors in different directions and on a variety of timescales. However, the way that the image is covered is not very predictable. So although this works well in practice for maps which are not much bigger than the array size, for much larger maps the Lissajous approach is not effective, because it can sometimes take

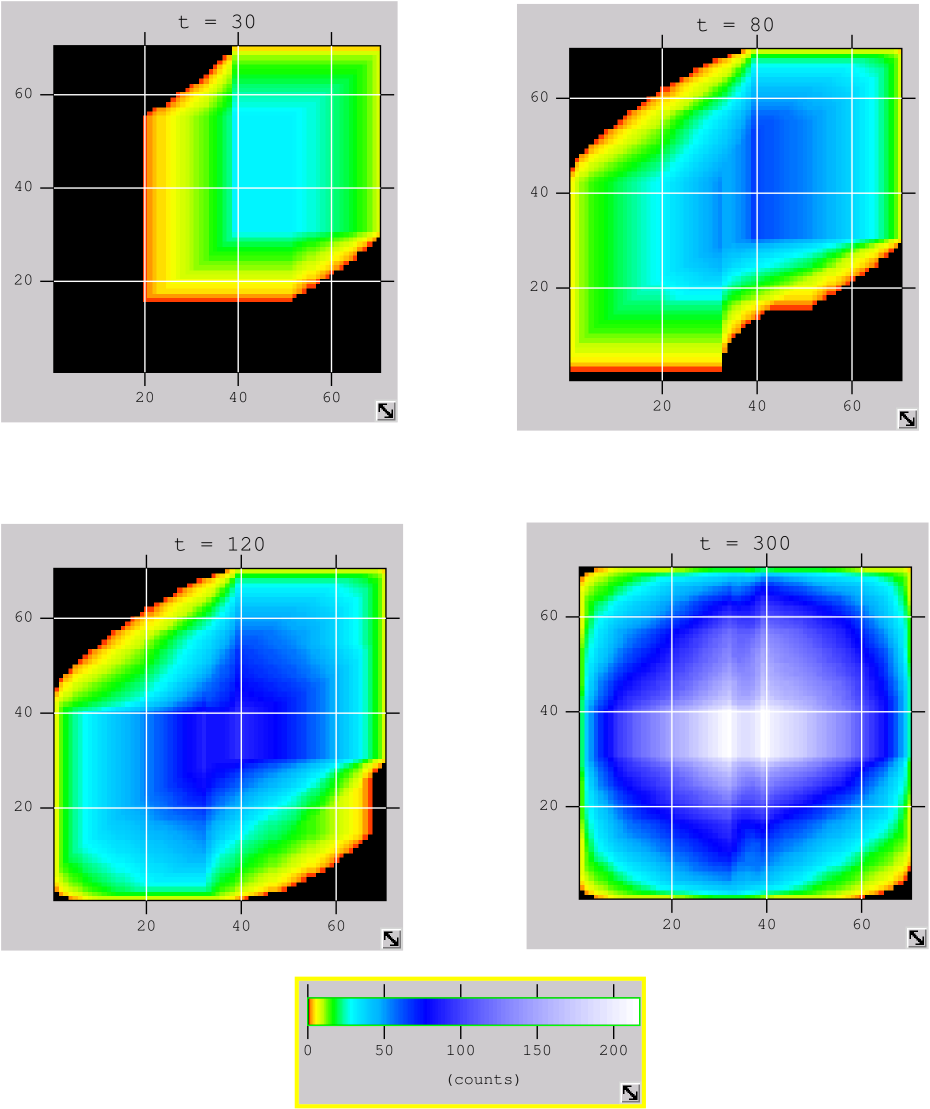

Figure 3: Simulation of an example of a Lissajous scan (see Fig. 2), showing the sky coverage as time evolves.

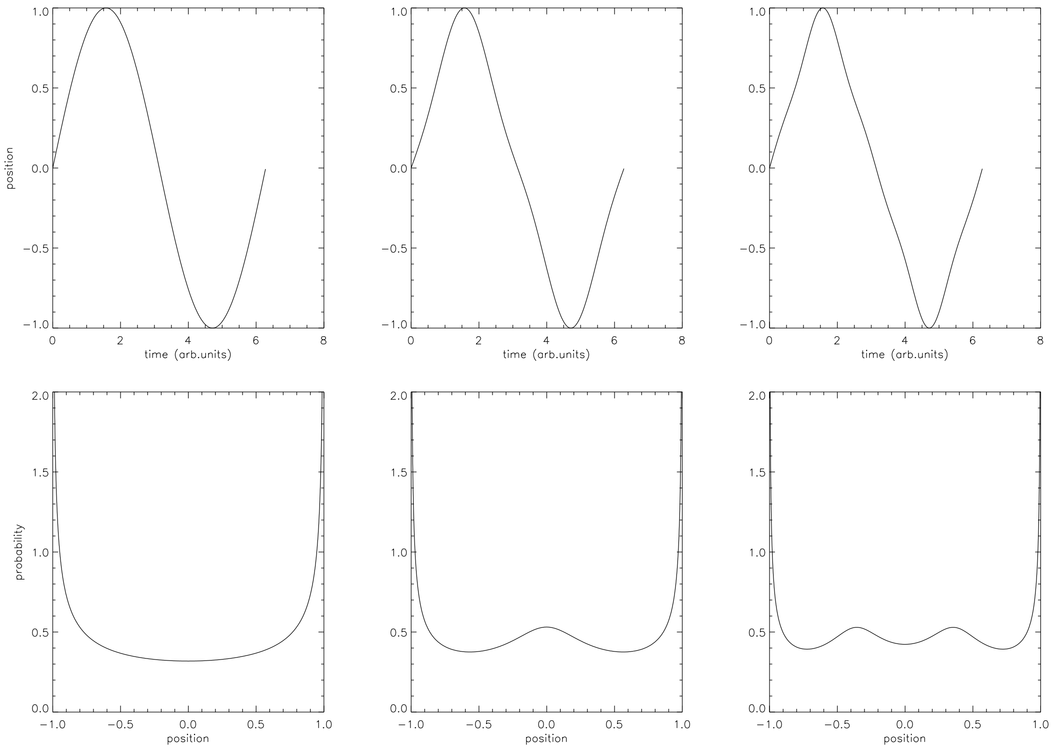

Figure 4: Investigating the effect of straightening out the scan pattern from a sinusoid. The top row gives one-dimensional scans as a function of time, and the bottom row gives the sky coverage, expressed as the probability distribution function of finding the ‘particle’ (our detector array) at a given position. This is an approximation to the pixel hit count for a very small array (e.g. a single detector, or a *very* large scan-map relative to the array size); however, for a non-negligible, extended array of equally-sensitive detectors, these PDFs need only be convolved with a top-hat function with width equal to that of the array. The first column corresponds to a single sine function; the next is the base sine function plus the next term in the Fourier expansion of a triangle wave (of period 2π on this scale); and the third column adds the third Fourier mode. Note the substantial increase in the amount of time spent at the map centre when only one Fourier mode is added to the base sinusoid. As more terms are added, the PDF will converge to a constant value of $\frac{1}{2}$. (The convergence is pointwise, however: the PDF *must* blow up at the edges, regardless of the number of Fourier terms, in order to keep a finite acceleration at all points.)

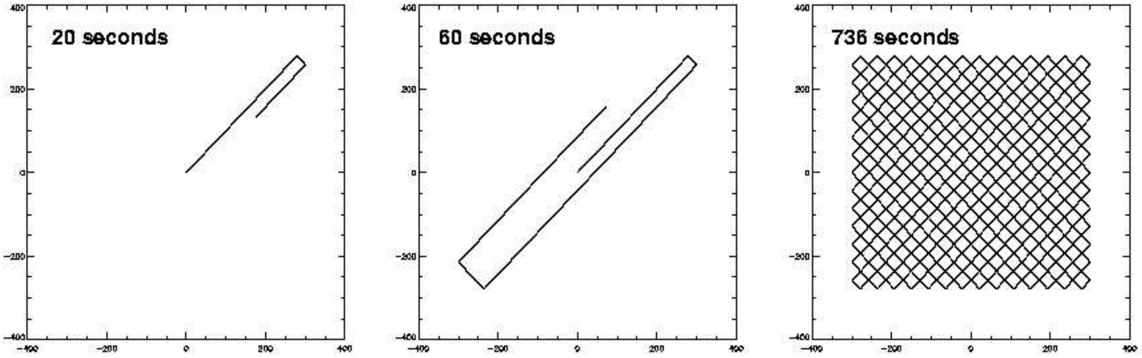

Figure 5: An example of a 'Pong' scan. This example (taken from the SHARC-II documentation) shows how the pattern is built up over time, starting near one diagonal, eventually passing close to the other diagonal and finally closing back at the starting position. This particular pattern has 14×13 diamonds in the entire image, and it is easy to see how these numbers would be different for a different choice of initial position.

a long time for the entire image to be covered.

4.3 Pong SCAN

For mapping a big area, several times larger than the SCUBA-2 array, the simplest idea is to scan along straight lines. With the requirement to change directions often, while continuously taking data, the best scanning approach is something which contains some of the positive features of both the Boustrophedon and Lissajous approaches. We call this the 'Pong scan' (and other people call it the 'box scan' or 'billiard ball scan'). One can think of this as the telescope position being a 'ball' bouncing around inside a box, with specular reflection at the walls. So imagine the telescope position being scanned along one direction, at some angle to the edge of the map, until it reaches the edge, when it bounces off and then continues until it reaches another side, and so on (see Fig. 5. The result is a series of cross-linked 'diamonds.' The size of these diamonds, and whether or not the pattern closes, depends entirely on the initial conditions chosen. It is clear that, for a square map, for example, if one started close to a diagonal and travelled at $45°$ to one of the sides, then the distance between neighbouring 'swaths' can be made arbitrarily small.

There are several elementary constraints with regard to these types of scan pattern in order to satisfy the criteria laid out in Section 3. First of all, the number of diamonds in the x-direction and that in the y-direction must not share any common factors. And secondly, one of the numbers must be even and the other odd. In fact this mode is mathematically identical to the Lissajous scan described above, with all the other Fourier modes brought in, in order to generate a saw-tooth function for $x(t)$ and $y(t)$.

For SCUBA-2, imagine that we scan at the angle of $\arctan(\frac{1}{2}) \simeq 26.5°$ (and for a rectangular array there is a 4-fold symmetry for this angle). This means that each row fills in between the pixels of the row in front. This will, in a simple way, make up for the fact the undersampling at $450\,\mu$m. In fact, for an array with a large number of rows (i.e. for SCUBA-2, but not for SCUBA) full sampling of the map will be achievable for almost any scan direction, *except* those which are parallel to the rows or columns of the array. For the sake of making a good cross-linked Pong pattern which completes rapidly, it is also necessary to avoid scan directions which are close to parallel to the edges of the region being mapped. To avoid the possibility of accidental undersampling (or never completing the map at all) it is probably best to fix the scan direction to one of those offered by $\arctan(\frac{1}{2})$, $\arctan(\frac{1}{3})$ (or possibly other angles, although this is probably enough choices) with respect to one of the axes. It would be preferable if this decision was made automatically as the default when the mode is selected at the telescope (although an override should be possible).

For redundancy purposes we would like each sky pixel to be measured at least twice in parallel scans. A total of 3 or 4 may be better, but there is obviously a trade-off here with the speed at which the map is made. It is also unclear whether one might want the coverage to be twice per sub-array, or twice for the whole set of arrays. All of these issues will have to be optimised when real data exist – the important thing is to have the options set up in advance so the optimal solutions can be found for different types of map.

If we assume that each part of the map should be covered twice by each sub-array, and that we are scanning at an angle of $\arctan(\frac{1}{2})$, then adjacent 'swaths' would be separated by $(4\,\mathrm{arcmin}) \times \sin(\arctan(1/2)) \simeq 1.8\,\mathrm{arcmin}$.

It is also simple to round off the corners in a Pong SCAN to avoid telescope acceleration or jerk constraints. The CSO avoids this for SHARC-II observations by using only the first 3 terms in the saw-tooth functions for $x(t)$ and $y(t)$.[1] This leads to a slightly undulating diamond pattern, which has no dramatic effect on the map-making.

Some work still needs to be done to implement this mode, which is the best guess strategy for large map-making projects of the sort being suggested for SCUBA-2 Surveys. The SHARC-II team have made a simple piece of code available to help choose the parameters for the commands which drive the telescope. For SCUBA-2 it will be necessary also to consider how these parameters are affected by orientation of the map (it may be necessary, for example, to restrict maps to being rectangular in RA,Dec coordinates), size of the map, orientation of Naysmith coordinates relative to RA,Dec, sky rotation during the scanning, etc.

4.4 Daisy SCAN

One further idea which might be useful, in particular for the commissioning phase of the instrument, would be to devise an *extremely* well cross-linked scheme, in which a central region of pixels is seen over and over by the array. This can be thought of in analogy to the *Planck* satellite observing mode, in which each circular scan on the sphere is linked through a small number of pixels at the North and South Ecliptic Poles.[**?**] An excellent overview of this mode is provided by Brian Mason for the 'Penn Array' at the Green Bank Telescope.[10]

A very important advantage of this SCAN strategy is that a bright source could be placed at the centre and used to correct for large systematic effects (larger than expected gain variations, say, or individual bolometer offsets or calibrations which have to be solved for using the map data themselves). It seems like a very wise idea to have such a SCAN variation ready for use with SCUBA-2 should the data reduction prove difficult during the early days of the instrument. The Daisy SCAN could conceivably even be used as a science mode for deep maps around bright sources, particularly if it turns out that there is a stronger than expected source of $1/f$ noise in the SCUBA-2 data.

A parametric description of this would be

$$\begin{aligned} x(t) &= r_0 \cos(\Omega t) \sin(\omega t) \\ \text{and} \quad y(t) &= r_0 \sin(\Omega t) \sin(\omega t), \end{aligned} \tag{3}$$

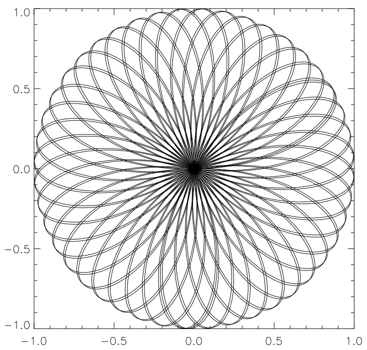

Figure 6: A sample Daisy scan. Note how all the paths cross near the centre of the image, where one could place a bright source in order to correct gain variations, for example.

which can be visualized as a basis vector rotating with angular velocity Ω, which modulated radially by a sinusoid at frequency ω. Again, if the ratio of these frequencies is rational then the result is periodic. The number and tightness of the 'petals' of the daisy-pattern can be set by varying ω and Ω, and the overall size of the circular region scanned depends on r_0. An example of a Daisy SCAN is shown in Fig. 6.

5 Conclusions

4 separate variants of SCAN mode have been outlined. Work still needs to be done to implement these on the JCMT for SCUBA-2. However, some comfort can be taken from the fact that the SCUBA-2 Project does not need to reinvent any wheels here, since we can draw on the direct experience of scan strategies already developed for existing array detectors at similar facilities around the world.

References

[1] C. Borys. Box Scan for SHARC-II. CSO telescope notes, URL: http://www.submm.caltech.edu/∼sharc/operating/boxscan.htm, 2003.

[2] C. Borys. Lissajous Scan for SHARC-II. CSO telescope notes, URL: http://www.submm.caltech.edu/∼sharc/operating/lissajous.htm, 2003.

[3] C. D. Dowell, C. A. Allen, R. S. Babu, M. M. Freund, M. Gardner, J. Groseth, M. D. Jhabvala, A. Kovacs, D. C. Lis, S. H. Moseley, T. G. Phillips, R. F. Silverberg, G. M. Voellmer, and H. Yoshida. SHARC II: a Caltech submillimeter observatory facility camera with 384 pixels. In *Millimeter and Submillimeter Detectors for Astronomy. Edited by Phillips, Thomas G.; Zmuidzinas, Jonas. Proceedings of the SPIE, Volume 4855*, pages 73–87, February 2003.

[4] B. D. Kelly. SCUBA-2 modes and data processing. SCUBA-2 Project SC2/ANA/S100/028, 2001.

[5] B. D. Kelly. SCUBA-2 scanmap simulation. SCUBA-2 Project SC2/ANA/S100/038, 2002.

[6] B. D. Kelly. SCUBA-2 noise-free DREAM simulations. SCUBA-2 Project SC2/SOF/S200/012, 2003.

[7] B. D. Kelly. DREAM noise simulations. SCUBA-2 Project SC2/SOF/S200/018, 2004.

[8] B. D. Kelly and W. D. Duncan. Application of DREAM observing to SCUBA-2. SCUBA-2 Project SC2/ANA/S100/006, 2001.

[9] R. S. Le Poole and H. W. van Someren Greve. DREAM: Dutch real-time acquisition mode for SCUBA. In *Proc. SPIE, Vol. 3357, Advanced Technology MMW, Radio, and Terahertz Telescopes, Thomas G. Phillips; Ed.*, pages 638–643, July 1998.

[10] B. Mason. Daisy Scan Mode for the GBT. Precision Telescope Control System PTCS Project Note 33.1, URL: http://wwwlocal.gb.nrao.edu/ptcs/ptcspn/ptcspn33/ptcspn33.pdf, 2003.

[11] M. Tegmark. CMB mapping experiments: A designer's guide. *Physical Review D*, 56:4514–4529, October 1997.

[12] H. W. van Someren Greve. DREAM algorithms for SCUBA-2. SCUBA-2 Project SC2/ANA/S100/046, 2002.

[13] E.L. Wright. Scanning and Mapping Strategies for CMB Experiments. astro-ph/9612006, 1996.